Image Transmission through Incoherent Optical Fiber Bundle: Methods for Optimization and Image Quality Improvement

O. DEMUYNCK, J.M. MENÉNDEZ
Escuela Técnica Superior de Ingenieros de Telecomunicación
UNIVERSIDAD POLITÉCNICA DE MADRID
Ciudad Universitaria, 28040 - MADRID
SPAIN
odemuynck@hotmail.com, jmm@gatv.ssr.upm.es

Abstract: - Artificial vision, in spite of all theoretical and practical progress accomplished during last thirty years, still cannot be employed technically in some hazardous and strong industrial areas, where conditions are such that cameras would not operate properly. Possible alternatives on such problem are the quite recent IP65 and IP67 industrial cameras, and associated connectors, protected by an anticorrosive, waterproof, and high temperatures resistive carcass employing a dedicated electronic, in addition robust to almost 3G accelerations. Nevertheless, such cameras are still very expensive compared to conventional industrial cameras and would still not be enough in hardest conditions (explosive gas or dust environment) or in electromagnetic interferences environments. A good alternative in extreme conditions is the use of optical fiber bundle. Since such cable only transmits light, they intrinsically have electromagnetic interferences immunity and, depending on the fiber material, could be exposed to very high temperature (over 1000ºC for sapphire fibers for example), could be employed in almost all corrosive environment, and are totally submersible. Nevertheless, the coherent optical fiber bundles are very expensive, and for large distances could be non-competitive facing the other hardware solutions (armor plating, electromagnetic interferences isolation). Thus, the best suitable option to develop a competitive system in those particular cases is the use of incoherent optical fiber bundle (IOFB), nowadays just employed for illumination tasks. Image transmission in this case is not direct but require a calibration step that we discuss in this paper. Improvement of the noisy resulting quality image is also exposed here, achieved by experimental post calibration methods.
We propose in this work a new calibration method of incoherent optical fiber bundle (IOFB) for image transmission purpose. Firstly, we present the calibration method (an enhancement of previously published calibration methods), some resulting reconstructed images and a discussion on its quality improvement employing simple denoising methods assisted by low pass filters (smooth filter, resizing method,…) . We finally depict the two new post calibration methods, and its associated noise generator physical phenomena we want to treat. Those two post calibration method are: correction of the input plane optical aberrations and extraction of a unique pixel (almost centered) for each fibers. We finally present some resulting images that demonstrate how it efficiently refine the reconstruction Look Up Table (LUT) used for the output image reconstruction improving image quality, image contrast but also reconstruction processing time.

Key-Words: Image transmission, incoherent optical fiber bundle, hazardous environment, calibration

1 Introduction

Image processing and artificial vision, two different technologies that belong to the field of Signal Processing, have experienced a huge evolution in the last decades. The use of those theories, and most of their future application, is mainly depending on computer science exponential improvement, but is already employed in almost every technological field, from medicine to multimedia. Such expansions generate a strong scientist and engineering interest, and multiply the diversity of implementation of system assisted by camera. The very special and dedicated machine vision application field we cover in this paper is the image transmission through IOFB (Incoherent Optical Fiber Bundle).

During the very recent years, previous studies already discussed the advantages and inconvenients of such system [1] [9] [5] [3]. The fact that IOFB only transmit light allows its use in strong industrial areas where electromagnetic interferences, high temperatures and/or humidity rate (until immersion over high pressures) can be reached, and much more since the previous examples just corresponds to a short list of environments where the use of conventional cameras is impossible. On the other

hand, employing a coherent optical fiber bundle, as in medicine for endoscopies, would result very expensive for building a complete high distances vision system. Of course, images transmitted by IOFB's are affected and distorted by external and internal effects. Externals, such as input lens distortion and optical aberrations. Internal, such as non-uniform illumination due to individual fiber transmission rates, and inside fiber color component mixing at the input plane. This last phenomenon is illustrated in figure 2, and is simply due to the fact that, even in a same sized fiber and pixel relation, the repartition of fiber is not the same as the compact array pixels repartition. The theoretical fiber repartition and the real fiber repartition is shown in the figure 1.

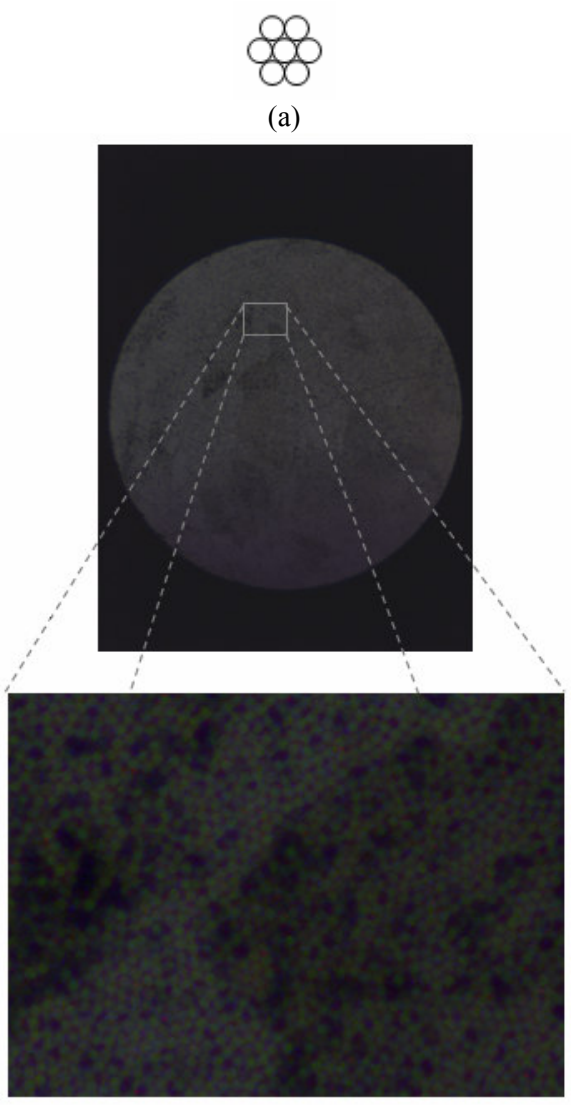

(a)

(b)

Fig.1: Optical fiber repartition in the IOFB. (a) A theoretical repartition sample. (b) Real repartition.

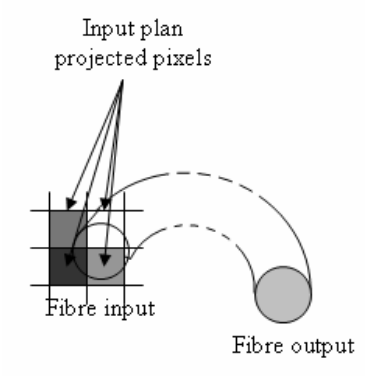

Fig.2: Information mixing phenomenon due to the elements repartition differences.

IOFB calibration for image transmission purpose has already been studied [2][3][4] and also been patented [8][6][7]. Time processing optimization and competitive algorithms has been successfully implemented, always employing a better hardware and dedicated optical devices. Nevertheless, the calibration system established in all those papers is still quite similar and none of those patents actually propose a real quality improvement, such as non-uniform light transmission correction, as it have been demonstrated in [4]. This is the main reason why no further applications have been published yet, basically because reconstructed image quality is still not enough to directly apply any image processing or computer vision technique. In deed reconstructed images are distorted by a strong noise, and causes further problems as it is exposed for example in [13], where the difference between a canny filter applied on a clean or a noisy image is shown. Some previous improvement in the reconstructed image is still required, and in this line some research should still be performed. Our work provides new solutions to this problem.

In this paper, we firstly present a novel calibration method, optimized in terms of output quality and processing time, compared to the two first proposals made in 2005 by [2][3]. This calibration method stems from previously experimented and patented ones [7] but include an intelligent processing variation that allows for a post calibration refinement and enhancement in the final image quality. Secondly, we show some reconstructed images, transmitted by a previously calibrated IOFB, and discuss the quality improvement produced by applying a denoising step (resizing method and a common smooth filter) on those reconstructed images. Finally, we propose a new two steps calibration method that improves the quality of image transmission, and explain the advantages of the calibration method variation.

2 Calibration method

In this section, we initially shortly detail the hardware used for the system. Afterwards, we describe the implemented calibration algorithm and compare it to previously implemented ones. To finish this section, we show some results obtained by our calibration process and compare some basic denoising method by correlating the reconstructed image with the original one.

2.1 Hardware employed for this calibration

Figure 3 represents a scheme of the implemented calibration setup.

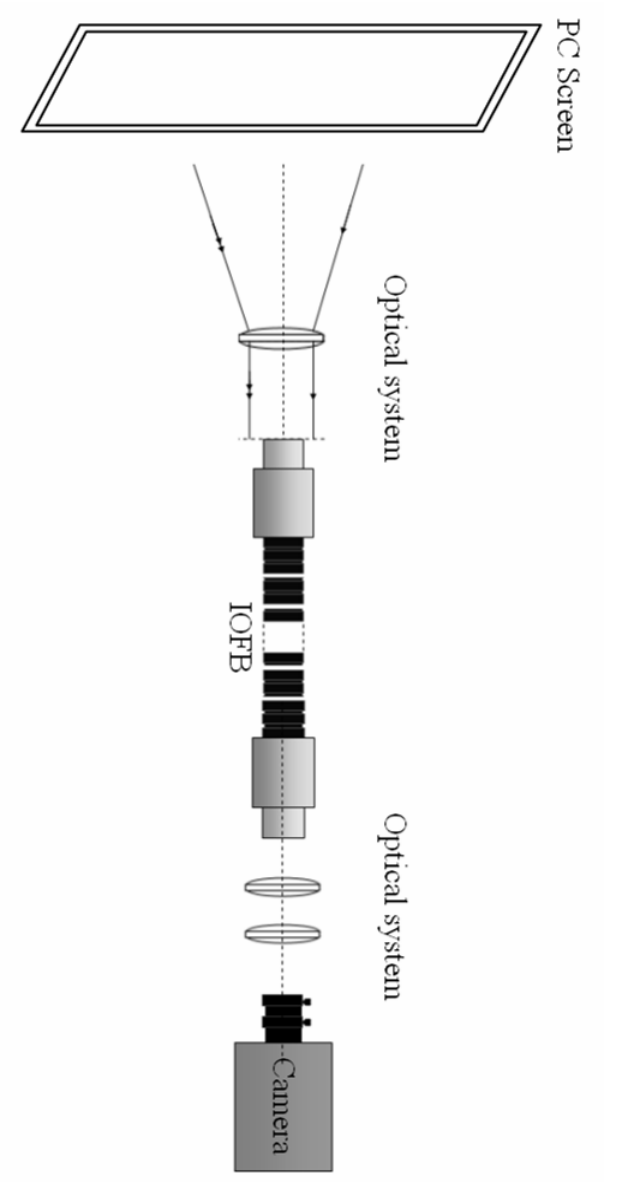

Fig.3: Calibration hardware setup.

The system is composed by a flat 17" PC screen configured with the maximum resolution (1280x1024 pixels) that emits the input. Optical systems are fixed on both side of the IOFB. The input optical setup fixes the field of view of the system, while the output one allows the output image to perfectly fit to the image sensor. The IOFB is a set of almost fifteen thousand individual optical fibers, and the output camera is a 6.6 Mega Pixels (3000x2208 pixels), 2/3" sensor camera, thus an almost 2200x2200 pixels square is used for this calibration since the IOFB output plane is observed as a non deformed circle that fit in a squared shape.

2.2 Operational principle

The algorithm starts with a black input image (none output pixel is registered), and progress horizontally and vertically with a step by step added thin white slice until the input image is completely white. Figure 4 represents two successive steps of this calibration process in the horizontal direction.

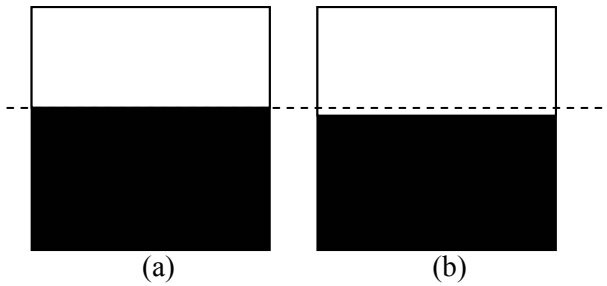

Fig.4: Successive steps of the calibration process. (a) step Sn, (b) step S_{n+1}.

With every new step, in which a new thin white slice is included in the input image, some new output pixels are registered, switching from dark to almost white, depending on a fixed threshold parameter referring to a new horizontal or vertical slice. The algorithm treats those registered pixels grouping the pixels that correspond in a horizontal and a vertical line pixels registration. Thus this pixels groups corresponds to the intersection of both horizontal and vertical slices. The slice size is given by an input parameter that finally fixes the reconstructed image precision. In deed, once the pixels are grouped, referring to a horizontal and vertical intersection, the mean value of this group of pixels will be use to refill a part of the reconstructed output image. This part of the reconstructed image is a squared group of pixels sized by the slice width parameter. To discuss this parameter, if it is too small, it will generate reconstructed image loss (each line being too thin for illuminating a fiber in most of the steps), and if this parameter is too big, it will result in a poor resolution and bad quality reconstructed image (since the square will be very big, including a huge group of output pixels not finely distributed). Pixels corresponding to

intersections are recorded in a reconstruction Look Up Table (LUT), and allow the distorted output image to be restructured and look like the original one.

The main difference with the closest calibration algorithm already proposed in [7] is that we are not just moving a horizontal of vertical white slice on a black background, but progressively completing the image until it gets fully white. This approach helps considerably in the optical aberration reducing post process depicted in the section 3.1, since we control the blurred effect direction. In deed, the optical aberration will just appear on the border between white and black areas, which is unique in our case, when in previous calibration method it appears twice.

2.3 Resulting reconstructed images

Two denoising filters have been implemented to reduce the noise of the reconstructed images. The first one relies on a simple spline interpolation. As explained in section 2.2, image resolution depends on the slice size. The method reduces the image size using a nearest neighbor interpolation by the slice size parameter (to avoid information repeating but not to distort the reconstructed image) and interpolates it back to its original size using splines to smooth the image. The second filter is quite similar since it applies the same process, but including and additional common smoothing step actually acting as a denoising filter. Some results of the reconstructed image using this calibration method and filtered by a spline interpolation scheme are shown in figure 5.

To assess and score the output quality and the global calibration process, we have correlated the reconstructed imaged with the original

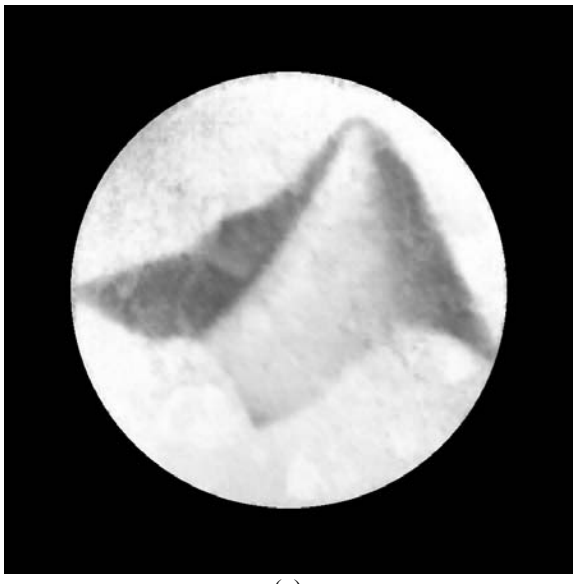

(a)

(b)

(c)

Fig.5: Reconstructed and spline interpolated images to correlate with the original ones.
(a) Matlab symbol, (b) Lenna, (c) A text.

The formula we used for the correlation is a common normalized correlation between two images. The equation of this correlation is given by:

$$score = \frac{\sum_{(i,j)} I_1(i,j) \times I_2(i,j)}{\sqrt{\sum_{(i,j)} I_1(i,j) \times I_1(i,j) \times \sum_{(i,j)} I_2(i,j) \times I_2(i,j)}}$$

Table 1 presents the computed scores of this calibration method using different filtering schemes.

Image	Method	correlation
Matlab	reconstructed	0.9929
	interpolated	0.9931
	smoothed	0.9931
Lenna	reconstructed	0.9779
	interpolated	0.9784
	smoothed	0.9785
Text	reconstructed	0.6121
	interpolated	0.6110
	smoothed	0.6098

Table 1: Computed correlation scores for each reconstructed image and used filtering method.

Of course, and before discussing those results, the correlation process strictly avoids the exterior circular black of the image that perfectly fit with the original images and would corrupt strongly the resulting scores. The correlation only treats the reconstructed image part.

The reconstructed images are also previously corrected following the study described in [4]. This processing usually does not correct the white values as it does with the black ones. We have observed a local illumination effect that increases all corrected values, probably due to the PC screen. According to that, we have centered the following discussion of those results on the Lenna case that is not affected by a white or black image background as it is the case for the Matlab symbol or the text respectively.

The reconstructed image quality score of 97,8% is very good for the Lenna case, even if we could criticize the use of this correlation method, since an absolute image subtraction could give a better idea of the image noise and some efficient tool could precisely quantify the image variation [12]. Nevertheless, and before applying any quality scoring process, it is very apparent that the image quality is very good, specially compared to previously shown results [1][2]. In all those cases, we note that the interpolation method significantly improve the results, whereas the smoothing filter looks not so interesting.

3 Post calibration

As listed in the abstract, the two phenomena (source of distortions) we decided to avoid are 1) the input optical aberrations caused by the small diameter lens and the imperfect focusing of the IOFB input plane (manually located), and 2) the weighted reconstruction due to the fact that some fibers appear bigger than others and so get an upper weight in the reconstruction step (in relation with the number of pixels included in the fiber projection on the image sensor), and also to the almost Gaussian light intensity distribution shape a fiber emits to the output plane. Figure 6 represents the optical aberration phenomenon.

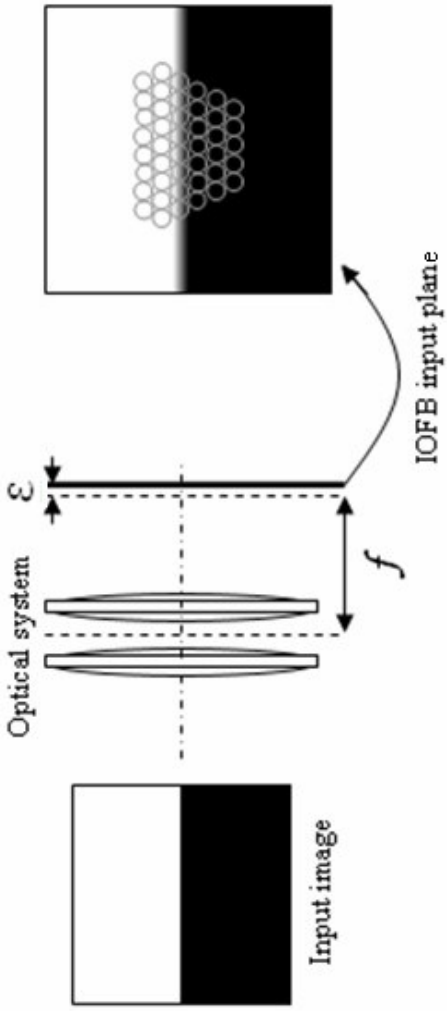

Fig.6: Optical aberration phenomenon at the input plane.

Figure 7 shows the individual optical fiber distortion phenomenon.

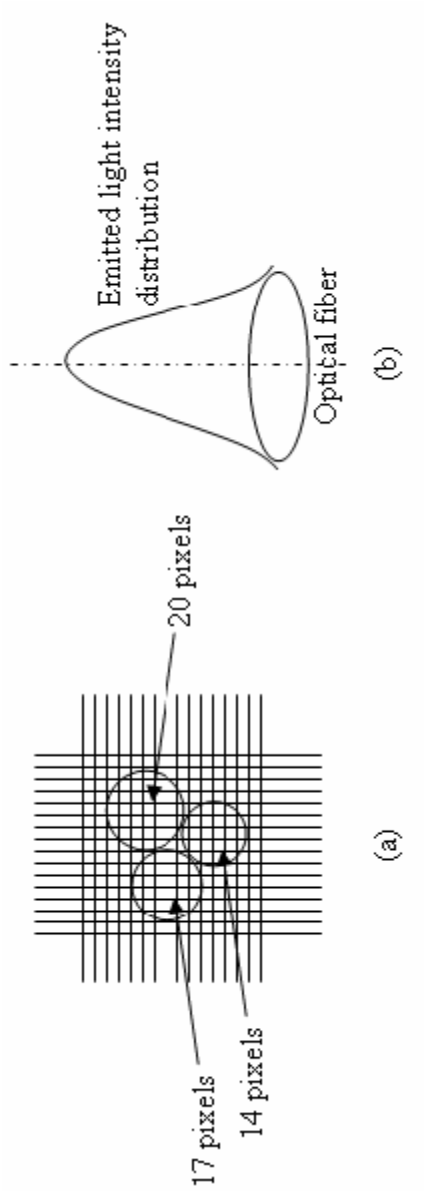

Fig.7: Individual optical fiber distortion phenomenon caused by (a) Fiber to pixels weighted reconstruction effect at the image sensor plane, and (b) Gaussian emitted light intensity distribution at the output of an individual fiber.

The two first problems (figure 6 and figure 7 (a)) are fundamental since they really introduce noise in the reconstructed image. In deed, the effect of optical aberration would cause registration from a fiber when it should not because of the illumination this smoothed border effect involve and the very thin diameter of the fiber. The effect of weighted reconstruction generates noise since some fiber (usually the fiber that has a better transmission rate) should not be more important in terms of information they transmit (even if illumination is not uniform, each fiber must have the same impact due to its spatial location). Nevertheless, because some fibers impact in more pixels or because some of them are even broken (which is quite frequent) this weighted average of values introduces strong distortions in the resulting reconstructed image. Finally the distortion shown in figure 7 (b) concerning the Gaussian distribution of the emitted light is corrected by the non uniform illumination process, and this problem is reduced to the extreme border pixels. Thus, selection of an approximately central pixel is enough to solve this problem. Nevertheless, this last phenomenon shown in figure 7 (b) is also a factor that concerns the problem of impacting pixels as in figure 7 (a). In deed, since each fiber has a different transmission loss rate, it could happen that some of them may be over illuminated, allowing to increase the diameter until about two additional pixels (one at both sides of the fiber along the diameter). Others would just illuminate fairly their own diameter, causing considerable variations of the relation number of pixels per fiber.

3.1 Optical aberration noise reduction

The process implemented to avoid the optical aberration effect is to reconstruct all the images used for the calibration process previously depicted and compare them to the original corresponding ones. Using an appropriate threshold we delete the strongly lighted fibers that appear over the separation line between black and white in the original images, and that should not have been selected at this step during the calibration process.

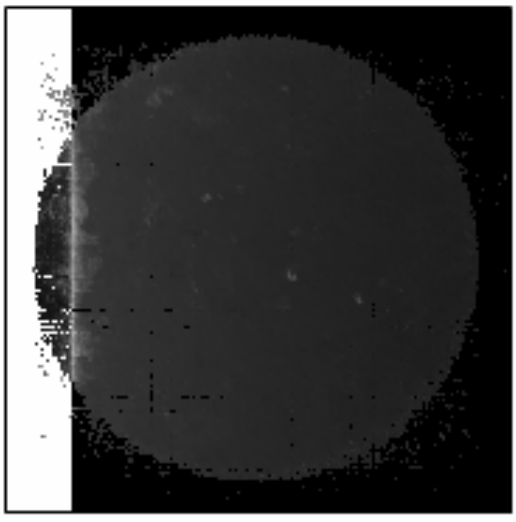

Fig.8: Step of the optical aberration noise reduction process.

Figure 8 depicts the basics of this algorithm. We observe the reconstructed image at a step of calibration in the vertical orientation and note the absolute difference with the original input image at the same step (white value corresponds to max difference). We observe at the border between white and black original image that the reconstructed image is affected by the optical aberration we already explained. Fixing a threshold we can discard some of those fibers in the reconstruction process.

3.2 One pixel fiber selection

The process implemented to select a central pixel in each input plane fiber projection is a bite more complicated than the way we solved the optical aberration issue. Some works already study this topic as in [6] and [10] where Hough transform circle detection and distance transform are used to get the fiber centers. Nevertheless, in those papers, the IOFB is not integrally treated since those methods require a mayor fiber projection size. Studies like [14] can be achieved by Hough circle detection since the detection of the eye iris is observed in almost half of the image. In addition, in [6], this fiber centre detection is not used to improve the calibration result, and so not to detect all the fibers, but to allow a reconstruction LUT to be newly computed to correct a probable IOFB rotation that would makes obsolete the originally calibrated reconstruction LUT. Other works focus the image sensor on a part of the output plane to observe, with a good enough scale, the fibers to apply such treatment, and concludes probabilistically on future improvements of the calibration process in case the technology allows to apply it on the whole output IOFB plane [10].

In this study, we implemented a new process to easily detect the fibers. First of all, we just consider the green component of the video signal, since red and blue components are noisier due to the transmission properties for those wavelengths in the fiber material. We process the IOFB region by region (the area of this region is fixed by an input parameter), but we do not require interpolation for the fiber detection. The reason why we process this way is the non uniform illumination problem that cannot be treated as previously done since it would also distort the non fiber image parts. For each selected part we use a Kapur automatic threshold [11] to efficiently binarize the selected area. We observed experimentally that this threshold should be a little bit increased to ensure we do not miss a fiber during the process. We implement a Blob analysis and select, as a fiber, those groups that respect the possible number of pixel for just one fiber. Too small number of pixels is considered as noise, and too big (usually at least twice) is considered as a group of fibers. The process then decreases the threshold in this area by canceling fibers already detected and iterating few times the algorithm until all groups are under the minimum number of pixel for a fiber.

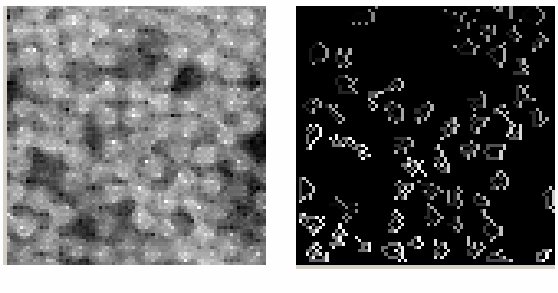

(a) (b)

Fig.9: Step of the central point fiber detection. (a) IOFB area selected. (b) Processed image.

Figure 9 shows (a) a selected area of the fiber, where about 70% of the fibers are already detected (b). The few following steps will detect the missing ones. We observe that the threshold value vary in a very thin range (about 15 iterations), what makes this procedure very fast. The centre of gravity of the pixels group selected as a fiber is then registered as the point to use in the image reconstruction process. Of course, moving the selected area by its own size makes some bordering fibers are always split, and so not detected. That is why the process is iterated integrally a second time with a bigger selected area chosen to not repeat this kind of error. To avoid the double detection of a same fiber during the second step (that probably would not perfectly repeat the same center of gravity), we mask each already detected fiber by a virtual fiber pattern. The resulting detection is represented in figure 10, where all the fibers are detected except one small sized and poor light transmission quality fiber.

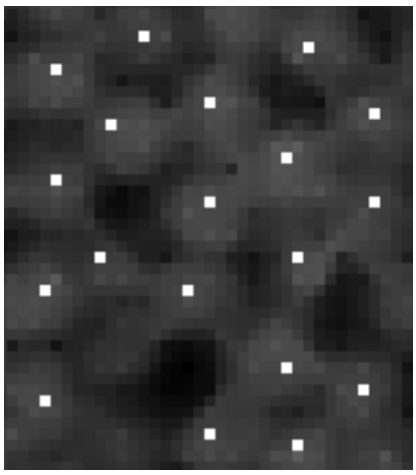

Fig.10: Result of the central point fiber detection.

Concluding on this first fiber detection result, we consider this processing as very efficient since 1) it never detects false fibers, 2) only miss some very small ones, 3) strong loss transmission rate fibers (probably neither registered in the calibration process due to the too small illumination), and 4) very small double detection of a same fiber (in case of a very good loss transmission rate fiber that even masked in the increased area size step still accepted as a big enough pixels group).

4 Experimental results

This section shows some resulting reconstructed images calibrated and post calibrated to observe the quality improvement we achieve. We finally discuss the improvement obtained by this calibration method, and the improvement obtained by both post calibration method in terms of computational cost. Nevertheless, and before showing any result, we show in the figure 11 the IOFB output image corrected following the non-homogeneous illumination algorithm proposed in [4].

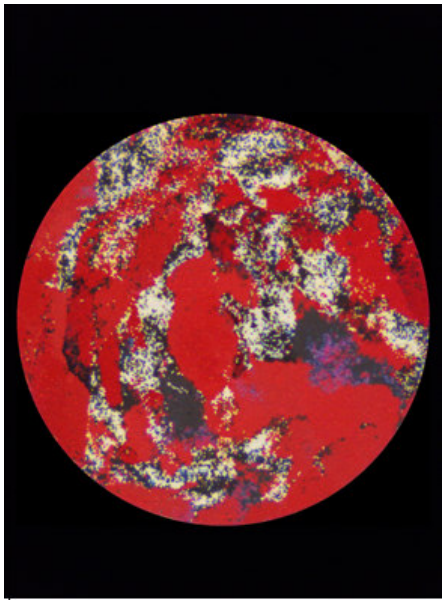

Fig.11: IOFB output image before reconstruction.

4.1 Optical aberration noise reduction

In figure 12, we observe different resulting reconstructed images obtained using different thresholds value for optical aberration cancellation. Figure 12 (a) corresponds to the original calibration reconstructed image. Figure 12 (b), (c), and (d) correspond to the reconstructed images using a refined LUT by the optical aberration reducing post calibration, with threshold values (referring to the gray level) equal to: 120, 100, and 80.

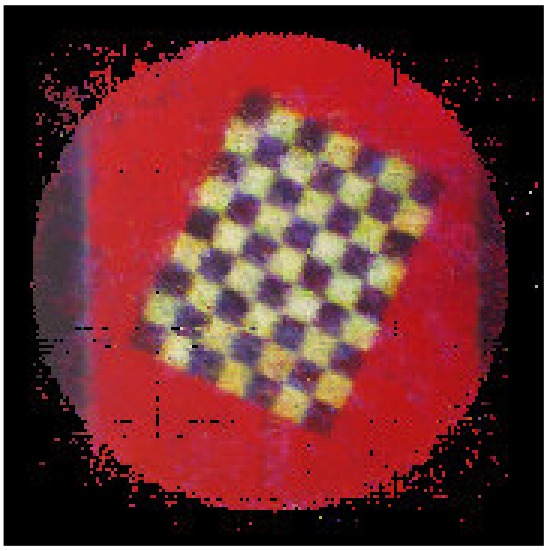

(a)

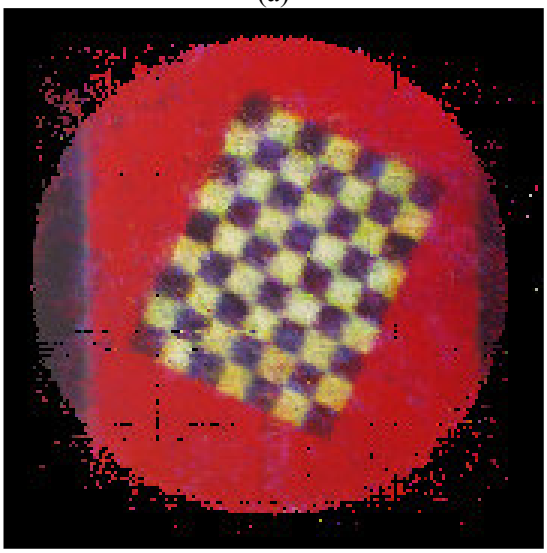

(b)

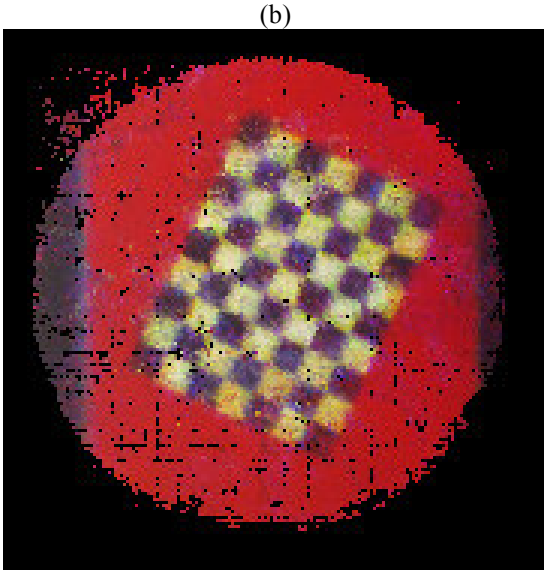

(c)

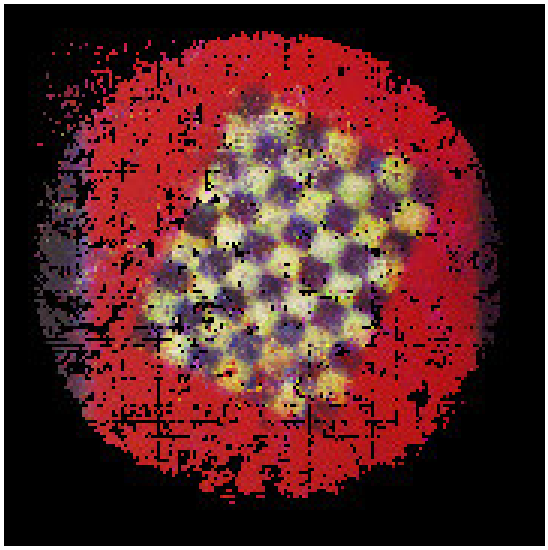

(d)

Fig.12: Result of the optical aberration reduction. (a) Original reconstructed image. Reconstructed image with a refined LUT using a threshold value equal to: (b) 120, (c) 100, (d) 80.

We observe that the corrected images are suffering quality degradation if the process is too selective with the previously registered fiber by the optical aberration phenomenon. Nevertheless, noise is clearly suppressed by this method since we easily observe the better external diameter definition of the IOFB. A good threshold value in the studied case is between 120 and 100 (respectively figure 12 (a) and (b)) since degradation in the reconstructed image can efficiently be corrected by an appropriate bilinear interpolation. This interpolation will actually just consider the neighbor that contain information and discard non-information neighboring pixels.

4.2 One pixel fiber selection

In figure 13 we observe two resulting reconstructed images. Figure 13 (a) corresponds to the original calibration reconstructed image, and figure 13 (b) corresponds to the reconstructed image using just the selected points in each fiber.

We observe that the corrected images are suffering quality degradation, but since such degradations can efficiently be corrected by a bilinear interpolation, we mainly note the image quality improvement of this post calibration. First of all, the noise is strongly reduced (as we can observe in each corner of the image, and as it is shown in figure 14 (a) and (b)), while the image in figure 14 (a) shows the upper left corners of the image in figure 13 (a), and the image in figure 14 (b) shows the upper left corners of the image in figure 13 (b). In addition, observing the selected part shown in figure 15 (a) and (b), we clearly note the contrast improvement and a sort of sharpening effect in the post calibrated image (that will be conserved even completing the missing image information with a bilinear interpolation since this interpolation would not affect the existing information but just complete the missing ones).

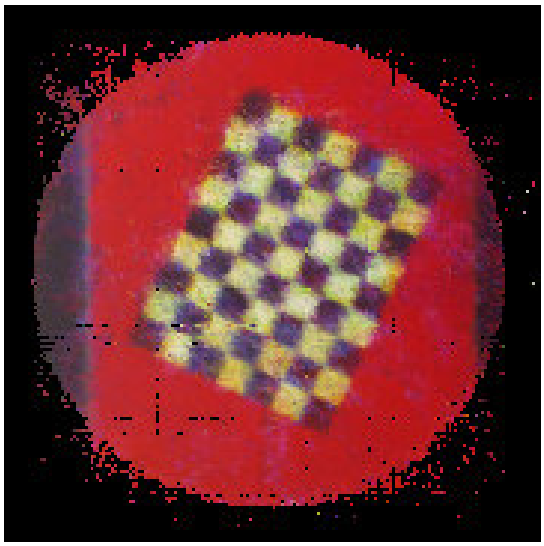

(a)

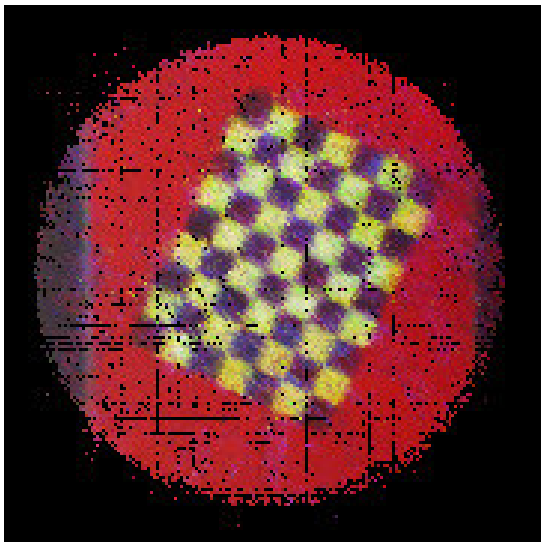

(b)

Fig.13: Result of the central point fiber detection. (a) Original reconstructed image. (b) Reconstructed image using the one point fiber selected.

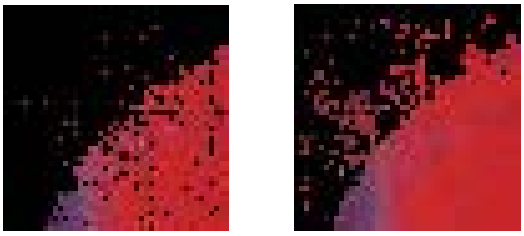

(a) (b)

Fig.14: Image quality improvement obtained by the central point fiber detection method.
(a) Original reconstructed image comparing area. (b) Reconstructed image using the one point fiber selected comparing area.

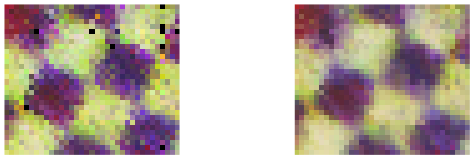

(a) (b)

Fig.15: Image quality improvement obtained by the central point fiber detection method.
(a) Original reconstructed image comparing area.
(b) Reconstructed image using the one point fiber selected comparing area.

5 Conclusion

We presented in this paper a new method to calibrate an IOFB, and a post processing applied to the reconstructed image that even improves reasonably an already good image quality. The last experimental results demonstrate the efficiency of both post calibration processing and, even more, the advantages of the one point fiber selection process. We conclude this study by the ideal combination of processes that should be chained to improve the image quality of reconstructed images. Firstly, to calibrate the cable with the depicted method, secondly to refine the LUT applying a soft optical aberration step to reduce the noise, reduce the reconstruction LUT to the one point per fiber selection process, and finally to interpolate the image to obtain it with the same resolution as the input image.

Running on an Intel Q6660 processor at 2.4Ghz computer, C programmed codes, and 6.6MPixels camera, the calibration is about 30 minutes (calibration images already captured), and the image reconstruction is about 17 seconds. The optical aberration reduction process is about 2 hours and the one point fiber selection takes approximately 1,5 hours. Of course this post calibration reduces considerably the reconstruction LUT initial composed by 4141169 pixels coordinates. In deed in the case shown in the figure 13 (b), we detected 47924 fibers and so reduce the reconstruction LUT that implies an acceleration factor of 86.4112. In this case the image reconstruction time is about 0.19 seconds, which is equivalent to a 5 frame/second camera. This result is very interesting since this FireWire 6.6 MPixels camera, in its full image transmission mode can only reach the 5 frames per second, so we could reconstruct the IOFB transmitted images without loosing any frame.

Extrapolation of this result sounds very exciting since a real-time cameras (almost 25 frames per second) dedicated to this application (squared sensor) could be close to 3 MPixels sensors and would actually allow a very similar quality result since those treatment would theoretically still working for a wide range of size variation (if the number of pixels per fiber decrease until a diameter of almost 4 pixels, the almost 13 pixels per fibers is very enough for a discrimination between an individual fiber and a group of fibers, or noise).

References:

[1] M.J. Tsai, J.S. Smith, J. Lucas, “Multi-fibre calibration of incoherent optical fibre bundles for image transmission”, *Trans. Inst. MC,* 15, 5, 1993, pp. 260-268.

[2] J. Gamo, O. Demuynck, Ó. Esteban, J.L. Lázaro, A. Cubillo, “Calibration of incoherent optical-fiber-bundle for image transmisión purpose”, *Proc. IADAT*, 2005.

[3] O. Demuynck, Ó. Esteban, J. L. Lázaro, J. Gamo, Á. Cubillo, “Transmisión de imagen por medio de un mazo de fibra óptica incoherente”, *Proc. OPTOEL’05*, 2005.

[4] O. Demuynck, J.L. Lázaro, Ó. Esteban, D. Pizarro “Non-Homogenous Illumination Correction of Calibrated Incoherent Optical-Fiber-Bundles for Image Transmission Purposes”, *IEEE International Conference on Mechatronics*, ICM 2006.

[5] C. Stephen, B. Robert, S.F. Chang, “High-Temperature Fiber Optic Imaging”, *Fiber and Integrated Optics*, 16, 4, 1997, pp. 387-405.

[6] B. Steven, R. McGowan, “Method and Apparatus for Using Non-Coherent Optical Bundles for Image Transmission” *Intel Corporation*, Patent No.: US 6,524,237 B1, 2003.

[7] H.E. Roberts, T. Huntsville, C.P. DePlachett, B.E. Deason, R.A. Pilgrim, T. Benton, H.S. Sanford, “Robust Incoherent Fiber Optic Bundle Decoder” *SRS Technologies*, Patent No.: US 6,587,189 Bl, Jul. 1, 2003.

[8] G.F. Dujon, A. Parker, A.J. Thomas, "Visual Image Transmission by Fibre Optic Cable", Publication Number: WO 91/06881, 1991.

[9] S. Zivanovic, J. Elazar, and M. Tomic, "Fiber-Optic Displacement Sensor", *Proc. International conference on microelectronics, miel'97*, 2, 1997, pp. 14-1.

[10] Fernandez P.R., Lazaro J.L., Gardel A., Esteban O., Cano A., "Calibration of Incoherent Optical Fiber Bundles for Image Transmission. Fibers Detection Process", *IEEE international symposium on Itelligent Signal Processing*, WISP 2007.

[11] Kapur J., Sahoo P., and Wong A., "A new method for graylevel picture thresholding using the entropy of the histogram", *Computer Graphics and Image Processing, 29(3):273–285.* , 1985.

[12] I.V. Gribkov, P.P. Koltsov, N.V. Kotovich, A.A. Kravchenko, A.S. Koutsaev, A.S. Osipov, A.V. Zakharov, "PICASSO 2 – a System for Performance Evaluation of Image Processing Methods"*, 5th WSEAS Int. Conf. on Signal Processing, Computational Geometry & Artificial Vision, Malta, September 15-17, 2005 (pp88-93).*

[13] G.N. Srinivasan, Dr. Shobha G "An Overview of Segmentation Techniques for Target Detection in Visual Images"*, 9th WSEAS International Conference on AUTOMATION and INFORMATION (ICAI'08), Bucharest, Romania, June 24-26, 2008.*

[14] JIANG Sai XIAO Gang GAO Fei LV Hui-qiang ZHANG Yuan-ming, "An Effective Iris Localization Method Through Enhancement of Boundary Detail"*, 5th WSEAS International Conference on Applied Computer Science, Hangzhou, China, April 16-18, 2006 (pp868-873).*